JOURNAL OF VIROLOGY, Jan. 2005, p. 1282–1295 Vol. 79, No. 2
0022-538X/05/$08.00+0 doi:10.1128/JVI.79.2.1282–1295.2005

Potential Nectin-1 Binding Site on Herpes Simplex Virus Glycoprotein D

Sarah A. Connolly,[1,2]* Daniel J. Landsburg,[1,2] Andrea Carfi,[3] J. Charles Whitbeck,[1,2] Yi Zuo,[1,2] Don C. Wiley,[4]† Gary H. Cohen,[1] and Roselyn J. Eisenberg[2]

Department of Microbiology, School of Dental Medicine,[1] and Department of Pathobiology, School of Veterinary Medicine,[2] University of Pennsylvania, Philadelphia, Pennsylvania; Istituto di Ricerche di Biologia Molecolare P. Angeletti, Rome, Italy[3]; and Department of Molecular and Cellular Biology, Howard Hughes Medical Institute, Harvard University, Cambridge, Massachusetts[4]

Received 21 June 2004/Accepted 4 August 2004

Four glycoproteins (gD, gB, gH, and gL) are essential for herpes simplex virus (HSV) entry into cells. An early step of fusion requires gD to bind one of several receptors, such as nectin-1 or herpesvirus entry mediator (HVEM). We hypothesize that a conformational change in gD occurs upon receptor binding that triggers the other glycoproteins to mediate fusion. Comparison of the crystal structures of gD alone and gD bound to HVEM reveals that upon HVEM binding, the gD N terminus transitions from a flexible stretch of residues to a hairpin loop. To address the contribution of this transition to the ability of gD to trigger fusion, we attempted to "lock" the gD N terminus into a looped conformation by engineering a disulfide bond at its N and C termini. The resulting mutant (gD-A3C/Y38C) failed to trigger fusion in the absence of receptor, suggesting that formation of the loop is not the sole fusion trigger. Unexpectedly, although gD-A3C/Y38C bound HVEM, it failed to bind nectin-1. This was due to the key role played by Y38 in interacting with nectin-1. Since tyrosines are often "hot spot" residues at the center of protein-protein interfaces, we mutated residues that surround Y38 on the same face of gD and tested their binding and functional properties. Our results suggest that this region of gD is important for nectin-1 interaction and is distinct from but partially overlaps the site of HVEM binding. Unique gD mutants with altered receptor usage generated in this study may help dissect the roles played by various HSV receptors during infection.

Herpes simplex virus (HSV) is a human pathogen that typically causes lesions on mucosal surfaces and spreads to the peripheral nervous system to establish life-long latency. The viral envelope contains at least 11 membrane glycoproteins, and 4 of these (gD, gH, gL, and gB) are essential for entry of HSV into cells and for cell-cell fusion (53, 59). An early and necessary step of this process involves the binding of gD to one of several known cell surface receptors (4, 53).

A recent study showed that gD engineered to bind an unrelated receptor can mediate virus entry into cells that bear that receptor (70). Based on this observation, the authors proposed that the only role of the gD-receptor interaction is to bring the envelope in juxtaposition to the plasma membrane. In many viral systems, however, entry is accomplished by the binding of a viral glycoprotein to a receptor, followed by a conformational change in that glycoprotein that triggers virus-cell fusion. Since gB, gH, and gL are conserved in all herpesviruses, it is widely accepted that they constitute the basic fusion machinery, but how their fusogenic activity is triggered is unknown. What varies among the herpesviruses are the viral receptor binding proteins and the specific cellular receptors. We hypothesize that one or more specific conformational changes occur in gD upon receptor binding that allow gH/gL heterodimer and/or gB to accomplish the fusion step (4, 20, 25, 53, 54).

Two of the molecules that serve as HSV entry receptors are nectin-1, a member of the immunoglobulin (Ig) superfamily of proteins (22, 35, 55) (Fig. 1A) and HVEM (for herpes virus entry mediator), a member of the tumor necrosis factor receptor family (33, 37, 43). Interestingly, these two structurally unrelated proteins each bind to gD with the same micromolar affinity (32, 53, 65). Nectin-1 mediates entry of all of the alphaherpesviruses tested so far (14, 22, 30, 31), while HVEM mediates entry of only HSV type 1 (HSV-1) and HSV-2 (43, 64). Some have proposed that nectin-1 represents the principal receptor for HSV in vivo due its expression on neurons, an important cell type in HSV pathogenesis (4, 52, 69). However, all of the approximately 60 HSV primary isolates that have been tested can use both HVEM and nectin-1 for entry (30). This suggests that both receptors may play important but distinct roles in HSV pathogenesis that have yet to be elucidated.

Previous studies have defined the gD and HVEM binding site (6, 12, 13, 62), but the precise location of the nectin-1 binding site on gD is currently unknown. Soluble forms of each receptor can block virus entry mediated by either receptor, suggesting that the two receptors bind to overlapping sites on gD (22). Further evidence for this is that certain monoclonal antibodies (MAbs) to gD block entry that is mediated by either receptor (31, 48). However, since other MAbs to gD prevent binding to nectin-1 but not to HVEM and vice versa, it is clear that a portion of the binding site for each receptor is distinct (31, 47). Furthermore, some gD mutations prevent HVEM binding without affecting nectin-1 binding (4, 53). One example is the rid1 mutation, a single amino acid change in gD present in a viral strain that was selected by its resistance to gD-mediated interference (15). This mutated form, gD-Q27P,

* Corresponding author. Mailing address: HHMI, Northwestern University, 2205 Tech Dr., Hogan 2-100, Evanston, IL 60208-3500. Phone: (847) 491-5432. Fax: (847) 491-2467. E-mail: connolly@northwestern.edu.
† Deceased.

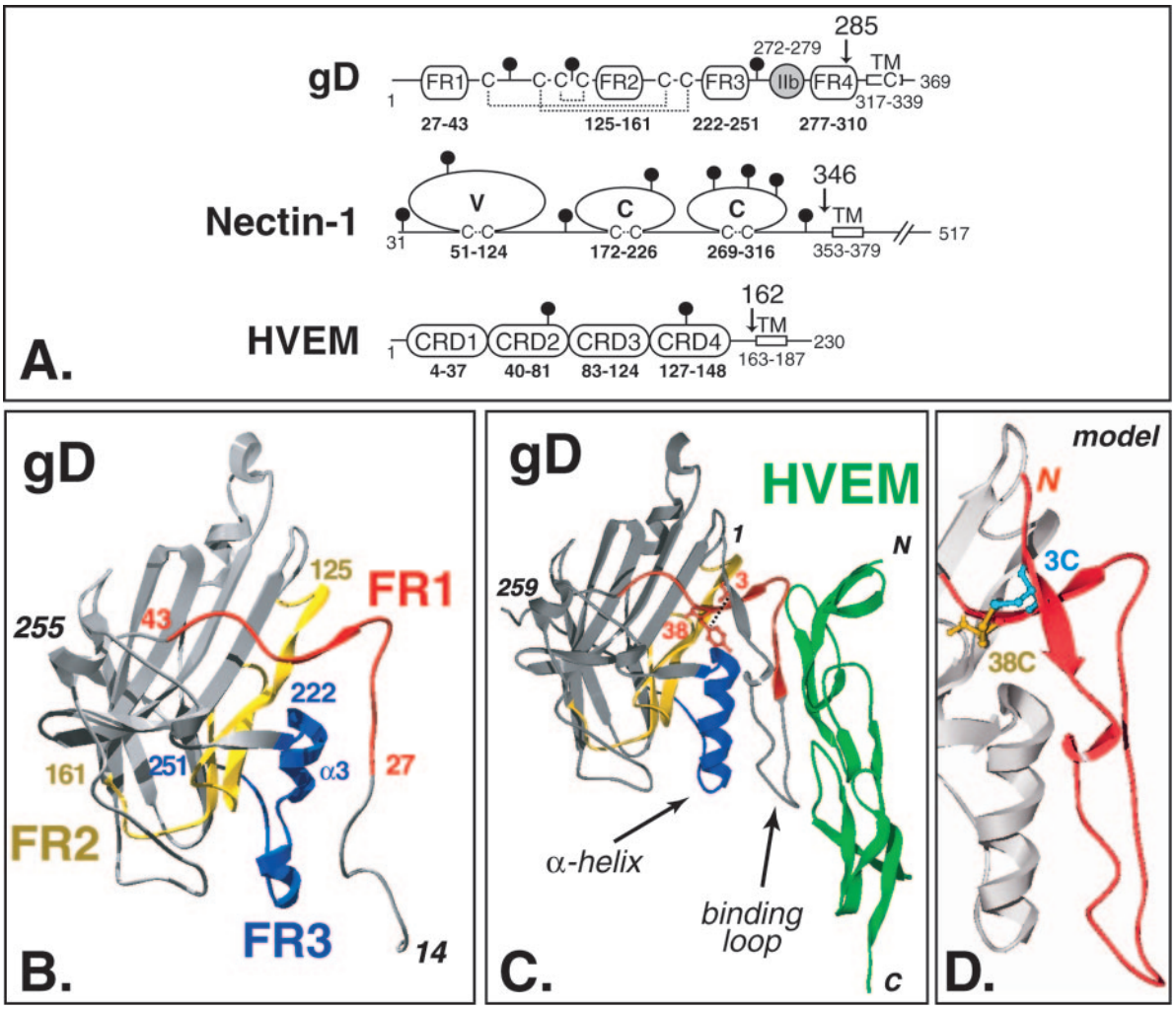

FIG. 1. Structural models of gD and receptors. (A) Diagram of full-length gD, nectin-1, and HVEM. The amino acid numbering begins with the first residue in the mature protein after signal sequence cleavage for gD and HVEM and the first residue of the precursor protein for nectin-1. The positions of N-glycosylation sites (lollipops) and transmembrane regions (TM) are indicated. The gD amino acids comprising each of four defined functional regions (FR) and the IIb MAb epitope (gray circle) are labeled. The disulfide bond pattern (dotted lines) and locations of cysteines (C) within gD are indicated. The nectin-1 amino acids comprising the variable-like (V) and constant-like (C) Ig domains are labeled, as are the disulfide bonds that define these domains (C--C). The break in the nectin-1 cytoplasmic tail indicates that it has been shortened to save space. The HVEM amino acids comprising each of the four cysteine-rich domains (CRD) are labeled. Arrows designate the sites of truncation for the purified proteins used to solve the crystal structures and/or in the following ELISA experiments. (B) Ribbon diagram of the crystal structure of unliganded gD. The N- and C-terminal residues observed in the crystal structure are indicated in black. The three FRs that were resolved in the crystal structure are colored, and the terminal residues of each FR are labeled. FR3 includes the α3 α-helix (blue). This structure represents a refinement of the previously described gD crystal structure (PDB accession no. 1L2G) (6). (C) Ribbon diagram of the interface between gD (red) and HVEM (green) (PDB accession no. 1JMA). The N and C termini of HVEM observed in the crystal structure are designated. The N- and C-terminal gD residues observed in the crystal structure are numbered 1 and 259, respectively, and the three gD FRs that were resolved are colored as in panel B. Arrows point to the N-terminal loop of gD that contacts HVEM (binding loop) and the extended α3 α-helix (blue) located behind the loop. Residues gD-A3 and gD-Y38 are shown, with a dashed line between them to indicate the position of the putative disulfide bond that might form if these residues were replaced with cysteines. (D) Model of a potential gD-A3C/Y38C conformation. gD residues 3 (blue) and 38 (yellow) have been artificially replaced with cysteine and linked by a disulfide bond that locks the N terminus of gD (red) in a loop conformation. All of the crystal structure graphics in this study were created using Swiss-PdbViewer (24) and POV-Ray software.

is unable to bind HVEM (64), and the rid1 virus cannot use this receptor (43). However, gD-Q27P binds nectin-1 with 10-fold-greater affinity than does wild-type gD (32).

Mapping the sites of gD mutations that disrupt nectin-1 binding should provide clues to the location of its binding site. However, to date, all of the gD mutants that lose nectin-1 binding also lose HVEM binding (29, 62), and so these mutants are not useful for dissecting the differences between the two binding sites.

The crystal structures of gD alone (Fig. 1B) and gD bound to HVEM (Fig. 1C) provide snapshots of gD in its pre- and postreceptor binding conformations (6). Comparison of these structures reveals two conformational differences that may contribute to the possible role of gD as a fusion trigger. Al-

though the structure of the gD–nectin-1 complex has not been solved, we speculate that binding of gD to nectin-1 may provoke similar conformational changes to provide a common triggering mechanism. One of the conformational changes that occur when gD binds to HVEM is a transition of the gD N terminus from a flexible stretch of amino acids to a hairpin loop that contacts HVEM (6). This conversion is accompanied by the formation of a long α-helix (α3) behind the N-terminal hairpin. The present project was originally designed to address dynamic aspects of the gD-HVEM interaction by examining the contribution of this N-terminal alteration of gD to its ability to trigger fusion.

Our approach was to "lock" the N terminus of unbound gD into a looped conformation by engineering a disulfide bond at the N and C termini of the hairpin loop. Previous studies have used this method of engineered disulfide bond cross-linking to address protein structure (1, 17, 18, 23). These studies were based on the concept that protein folding governs disulfide bond formation, and not vice versa (58). Thus, we substituted cysteine residues for two amino acids at the ends of the hairpin loop that are close enough to form a disulfide bond when gD is bound to HVEM (Fig. 1D).

The mutant containing this extra pair of cysteine residues was still able to bind HVEM and use it as a receptor in cell fusion assays. However, it was unable to trigger cell fusion in the absence of a functional gD receptor, suggesting that formation of the hairpin loop does not serve as the sole fusion trigger. Unexpectedly, this mutant was unable to bind nectin-1. The unique properties of this and other mutants led us to identify a site on gD that is critical for its interaction with nectin-1.

(This work was presented by S. A. Connolly in partial fulfillment of the requirements for the degree of Doctor of Philosophy at the University of Pennsylvania, Philadelphia, 2003.)

MATERIALS AND METHODS

Cells and viruses. 293T cells and mouse L cells were grown in Dulbecco's minimal essential medium (DMEM) supplemented with 10% fetal calf serum (FCS). B78-H1 mouse melanoma cells (39) were grown in DMEM supplemented with 5% FCS. These cells do not express any gD receptors but can be made permissive to HSV entry by transfection with a gD receptor. B78-H1-A10 cells and B78-H1-C10 cells were derived from B78-H1 cells to stably express human HVEM and nectin-1, respectively (39), and were grown in DMEM supplemented with 10% FCS and 500 μg of G418/ml. CHO-K1 cells were grown in Ham's F-12 medium supplemented with 10% FCS. CHO-HVEM12 (57), CHO-R3A, and CHO-R2 cells were derived from CHO-K1 cells to stably express human HVEM, nectin-1, and nectin-2, respectively, and were grown in Ham's F-12 medium supplemented with 10% FCS and 250 μg of G418/ml. CHO-IEβ8 cells (43) carry *lacZ* under the ICP4 promoter. M1A and M3A cells (32) were derived from CHO-IEβ8 cells to stably express human HVEM and nectin-1, respectively. These cells were grown in Ham's F-12 medium supplemented with 10% FCS, 150 μg of puromycin/ml, and 250 μg of G418/ml.

HSV-1 strain KOS was used as the wild-type virus. The gD-null virus, HSV-1 KOS-gDβ, carries *lacZ* in place of the coding region for gD under the control of the gD promoter (15). It was propagated on VD60 cells as described previously (34). VD60 cells were derived from Vero cells to express gD under control of its own promoter and were grown in DMEM supplemented with 5% FCS.

PAbs and MAbs. Rabbit polyclonal antibody (PAb) serum R7 was raised against HSV-2 gD and cross-reacts with HSV-1 gD (28). Anti-gD MAbs that recognize linear epitopes include DL6, which binds gD residues 272 to 279 (16, 28), and 1D3, which binds residues 11 to 19 (7, 10, 19). Anti-gD MAbs used that recognize discontinuous epitopes included DL2 (11), HD1 (44, 50), DL11 (11, 44), and AP7 (7, 42). IgG was purified from rabbit serum or mouse ascites fluid using HiTrap protein G 1-ml columns (Amersham Pharmacia Biotech).

Production and purification of soluble receptors. Procedures have been described elsewhere for the production and purification of the truncated ectodomains of HVEM (HVEM200t), nectin-1 (HveC346t), and nectin-2 (HveB361t) expressed by recombinant baculovirus-infected insect cells (31, 60, 64).

Construction of mutant gD molecules. The plasmid pSC390 was previously described (12) and encodes gD from HSV-1(KOS) in the pcDNA3.1 vector. We generated gD mutants using the QuikChange site-directed mutagenesis kit (Stratagene Cloning Systems). Briefly, primers designed to mutate individual gD residues were used to amplify the entire pSC390 plasmid by PCR. The reaction products were then treated with DpnI to digest methylated template DNA and used to transform competent bacteria (Invitrogen One-Shot Top10F′). We verified the mutations by sequencing the entire gD gene. With few exceptions, we changed particular amino acids to alanine. Substitution with alanine removes the majority of the original residue's side chain atoms, and this amino acid is found in many secondary structures in both exposed and buried positions (61). The 19 plasmids were named as follows: gD-V37A (pDL537), gD-Y38F (pDL505), gD-Q132A (pDL540), gD-T213A (pDL542), gD-S216A (pDL543), gD-R222A (pDL564), gD-F223A (pDL546), gD-R36A (pDL536), gD-H39A (pDL539), gD-G218A (pDL563), gD-L220A (pDL544), gD-R134A (pDL541), gD-D215A (pDL562), gD-P221A (pDL545), gD-Y38A (pDL504), gD-Y38C (pDL508), gD-A3C/Y38C (pDL490), gD-D30A (pDL449), and gD-Q27P (pDL491).

Syncytium formation assay. B78-H1, B78-H1-A10, or B78-H1-C10 cells growing in 24-well plates were transfected with plasmids encoding gB, gH, gL, and either wild-type gD or gD-A3C/Y38C. Aliquots of 250 ng/well of each plasmid and 5 μl of GenePORTER reagent (Gene Therapy Systems)/well in DMEM were added to the cells for 3 h, followed by addition of an equal volume of DMEM containing 20% FCS. Cells were incubated overnight at 37°C, fixed with methanol, stained with Giemsa (Gibco-BRL) for 10 min, and scored for syncytium formation by microscopy. This assay was repeated at least twice for each cell type with consistent results.

Enzyme-linked immunosorbent assay (ELISA). 293T cells growing in 12-well plates were transfected with the gD plasmids or empty vector, using 2 μg of DNA/well and 10 μl of GenePORTER/well for 3 h followed by addition of an equal volume of DMEM containing 20% FCS. Cells were incubated overnight at 37°C and then harvested in extraction buffer (10 mM Tris, 150 mM NaCl, 10 mM EDTA, 1% NP-40, 0.5% sodium deoxycholate, 1 mM phenylmethylsulfonyl fluoride; pH 8) supplemented with 1× Complete protease inhibitor (Roche).

We used a capture ELISA to normalize the amount of gD in the 293T extracts as previously described (12). Briefly, ELISA plates were coated with DL6 IgG (overnight at 4°C) and then exposed to blocking solution (phosphate-buffered saline [PBS] containing 5% nonfat dry milk and 0.2% Tween 20) for 1 h. Various dilutions of cell extracts containing gD were added for 2 h at room temperature (RT). Captured gD was detected with PAb R7 IgG followed by goat anti-rabbit antibody coupled to horseradish peroxidase. Plates were rinsed with 20 mM citrate buffer (pH 4.5), 2,2′-azinobis(3-ethylbenzthiazolinesulfonic acid) (ABTS) peroxidase substrate was added, and the absorbance at 405 nm was recorded using a microtiter plate reader. The level of gD in each extract was normalized by dilution in extraction buffer, and the normalization was confirmed by repeating the capture ELISA.

To assess receptor binding of the gD mutants, ELISA plates were coated overnight with soluble receptors (4 μg of HVEM/ml, 10 μg of nectin-1/ml, or 10 μg of nectin-2/ml), exposed to blocking solution for 1 h, and incubated for 2 h at RT with normalized cell extracts. Bound gD was detected as described above. Percent binding was defined as follows: $\{[A_{405(\text{mutant})} - A_{405(\text{vector})}]/[A_{405(\text{wildtype})} - A_{405(\text{vector})}]\} \times 100$. This assay was repeated at least three times for each form of gD.

Quantitative fusion assay. To detect cell-cell fusion, we used a luciferase reporter assay (12, 49, 51). Briefly, effector CHO-K1 cells were grown in 96-well plates and transfected with plasmids encoding T7 RNA polymerase, gB, gH, gL, and one of the gD mutants described above. Transfections were performed in triplicate. To prepare receptor-bearing target cells, CHO-HVEM12, CHO-R3A, or CHO-R2 cells growing in six-well plates were transfected with a plasmid encoding the firefly luciferase gene under control of the T7 promoter. After 6 h at 37°C, the transfection mixes were replaced with fresh medium. After overnight incubation at 37°C, target cells were trypsinized, added to the effector cells, and incubated at 37°C. At 20 h post-cocultivation, cells were washed with PBS, lysed in reporter lysis buffer (Luciferase assay system; Promega), and frozen. To measure the extent of fusion, samples were mixed with luciferase substrate (Promega) and immediately assayed for light output using a Luminoskan Ascent system (Thermo Labsystems). Plasmids encoding the firefly luciferase gene (pT7EMCLuc), T7 RNA polymerase (pCAGT7), gB (pPEP98), gH (pPEP100), and gL (pPEP101) were gifts of P. Spear (49, 51). This assay was repeated at least three times for each mutant.

Complementation assay. The complementation assay was performed as previously described (7, 12, 46). Briefly, L cells were transfected with pSC390, pDL490, or pcDNA3.1. After 3 h, an equal volume of DMEM containing 20% FCS was added. After an overnight incubation at 37°C, cells were infected with HSV-1 KOS-gDβ. After 2 h at 37°C, the medium was removed and extracellular virus was inactivated by a 1-min exposure to sodium citrate buffer at pH 3.0. Fresh medium was added, and the cells were incubated at 37°C overnight. At 24 h postinfection, plates were subjected to three freeze-thaw cycles and cell lysates contained the complemented virus. The virus preparations were then cleared of cell debris in a microcentrifuge and stored at −80°C.

To detect HSV entry into cells expressing defined receptors, we modified a previously described entry assay (32). Briefly, M1A or M3A cells growing in 96-well plates were exposed to serial dilutions of the lysates containing complemented virus. After an overnight incubation at 37°C, the cells were washed with PBS and lysed in DMEM containing 0.5% NP-40. β-Galactosidase activity in the lysate was measured by adding substrate (chlorophenol red-β-D-galactopyranoside; Boehringer Mannheim), reading the absorbance at 570 nm at multiple times using a microtiter plate reader, and recording the mean slopes. Percent complementation was defined as follows: $[(\text{slope}_{\text{mutant}} - \text{slope}_{\text{vector}})/(\text{slope}_{\text{wild type}} - \text{slope}_{\text{vector}})] \times 100$. This assay was repeated at least three times.

CELISA. To detect gD expression on cells, we used two versions of a previously described cellular ELISA (CELISA) (12, 21, 40). To determine the amount of gD on cells used in the fusion assay, one 96-well plate of effector cells was fixed in 3% paraformaldehyde (PFA) for CELISA and a duplicate plate was used for fusion. For the complementation assay, L cells were transfected and infected with gD-null virus as described above. The cells were replated 24 h postinfection on 96-well plates, incubated overnight at 37°C, and fixed in 3% PFA. For both assays, fixed cells were rinsed with 50 mM NH_4Cl to quench residual PFA, rinsed twice with PBS, and incubated with PAb R7 IgG diluted in DMEM–5% FCS for 1 h at RT (10 μg of IgG/ml for effector cells and 10-fold dilutions starting at 80 μg of IgG/ml for the L cells). The cells were rinsed with PBS three times and incubated for 1 h at RT with goat anti-rabbit antibodies coupled to horseradish peroxidase. Following another three PBS washes, cells were rinsed with 20 mM citrate buffer (pH 4.5). ABTS peroxidase substrate (Moss, Inc.) was added, and the absorbance at 405 nm was recorded using a microtiter plate reader. These assays were repeated at least twice.

Dot blot analysis of antibody binding to gD mutants. Cell extracts containing normalized amounts of the mutant forms of gD were spotted onto nitrocellulose using a dot blot apparatus (Schleicher & Schuell). Blots were incubated in blocking solution, reacted with various MAb IgGs or R7 PAb IgG, and incubated with secondary antibody (goat anti-mouse or goat anti-rabbit) coupled to horseradish peroxidase. Blots were washed with PBS containing 0.2% Tween 20 and visualized by enhanced chemiluminescence (Amersham)

RESULTS

gD undergoes conformational changes when bound to HVEM. In the crystal structure of gD bound to HVEM (PDB accession no. 1JMA) (6), all of the HVEM contact residues are within an N-terminal hairpin loop (amino acids 1 to 37) of gD (Fig. 1C). In a crystal structure of gD alone (PDB accession no. 1L2G) (6), the N terminus of gD does not bend at residue 21 to form a hairpin loop. Rather, residues 1 to 13 are disordered, suggesting that this portion of gD is flexible (Fig. 1B). Moreover, the α3 α-helix (residues 224 to 240), which is located behind the N-terminal hairpin in the complex, forms a kink at residues 232 in the structure of gD alone. Thus, as a result of binding to HVEM, gD undergoes a large conformational change at its N terminus that is accompanied by complete formation of the long α3 α-helix.

Can an altered form of gD mediate fusion in the absence of receptors? We hypothesized that one or both of the conformational changes in gD that occur upon HVEM binding might trigger the next steps of entry and fusion that are carried out by gB and gH/gL. We further hypothesized that if formation of the N-terminal loop served as a fusion trigger, creation of a gD mutant that assumes this structure in the absence of receptor may result in a molecule that mediates receptor-independent fusion. When HVEM is bound to gD, the side chain C_β of alanine 3 and tyrosine 38 face one another and come into proximity at a distance of 4.7 Å (Fig. 1C). Thus, we anticipated that cysteine residues introduced at these two positions should be able to form a disulfide bond and thereby lock the N terminus into a hairpin loop (Fig. 1D). Such a strategy has been applied to several other proteins (1, 17, 18, 23). The resulting mutant, gD-A3C/Y38C, was cloned into an expression vector and sequenced to verify the mutations.

We tested gD-A3C/Y38C function in a syncytium formation assay. B78-H1 mouse melanoma cells lacking any receptors for gD were transfected with plasmids encoding gB, gH, gL, and either wild-type gD or gD-A3C/Y38C. Since no syncytia were detected in either case (Fig. 2A), we conclude that gD-A3C/Y38C was unable to mediate fusion of the B78-H1 cells in the absence of receptor. Assuming that the 3–38 disulfide bond was formed in the mutant, these data suggest that formation of the gD N-terminal loop in the absence of receptor does not allow for triggering of fusion. As controls, we carried out the same transfections on B78-H1 cells stably expressing either HVEM (A10) or nectin-1 (C10). These cells form large syncytia within 48 h posttransfection (3, 41). A10 cells expressing gB, gH, gL, and either wild-type or the mutant gD formed syncytia (Fig. 2B). This result showed that gD-A3C/Y38C was expressed on the cell surface and was functional.

Interestingly, when the same transfections were carried out on nectin-1-bearing cells, wild-type gD mediated syncytium formation as expected but, unexpectedly, gD-A3C/Y38C failed to mediate fusion (Fig. 2C). This result identified gD-A3C/Y38C as a gD mutant capable of fusing HVEM-bearing cells but not nectin-1-bearing cells. Since this represents a unique receptor usage phenotype, we further analyzed the receptor binding properties of the mutant protein.

gD-A3C/Y38C binds to HVEM but not to nectin-1. To verify the receptor binding phenotype of gD-A3C/Y38C implied by the fusion assay, we investigated the binding properties of the protein. We employed an ELISA on extracts prepared from 293T cells transfected with plasmids encoding the wild-type or mutant form of gD (12). We used 293T cells because gD expression is high in these cells and this permits more accurate determinations of receptor binding than can be achieved using transfected B78-H1 cells. gD levels were normalized by a previously described capture ELISA (12) (Fig. 3A). Extracts were then diluted to contain equivalent amounts of gD.

Various amounts of normalized cell extracts were added to ELISA plates coated with soluble nectin-1 or HVEM (31, 64). Bound gD was detected with anti-gD PAb IgG. While the mutant gD-A3C/Y38C bound as well as wild-type gD to HVEM, it did not bind detectably to nectin-1 (Fig. 3B and C), confirming the results predicted by the fusion data (Fig. 2). Thus, gD-A3C/Y38C fails to use nectin-1 as a receptor because it fails to bind to it. This mutant also did not bind nectin-2, nor did it use this protein as a receptor for fusion (data not shown). Remarkably, this is the first mutant identified with this phenotype.

Additional gD-Y38 mutants provide information about the location of the nectin-1 binding site on gD. One possible reason why gD-A3C/Y38C failed to bind nectin-1 is that a mutation altered a critical residue within the binding site. Yoon et al. (68) showed that mutants lacking residues between 7 and 32

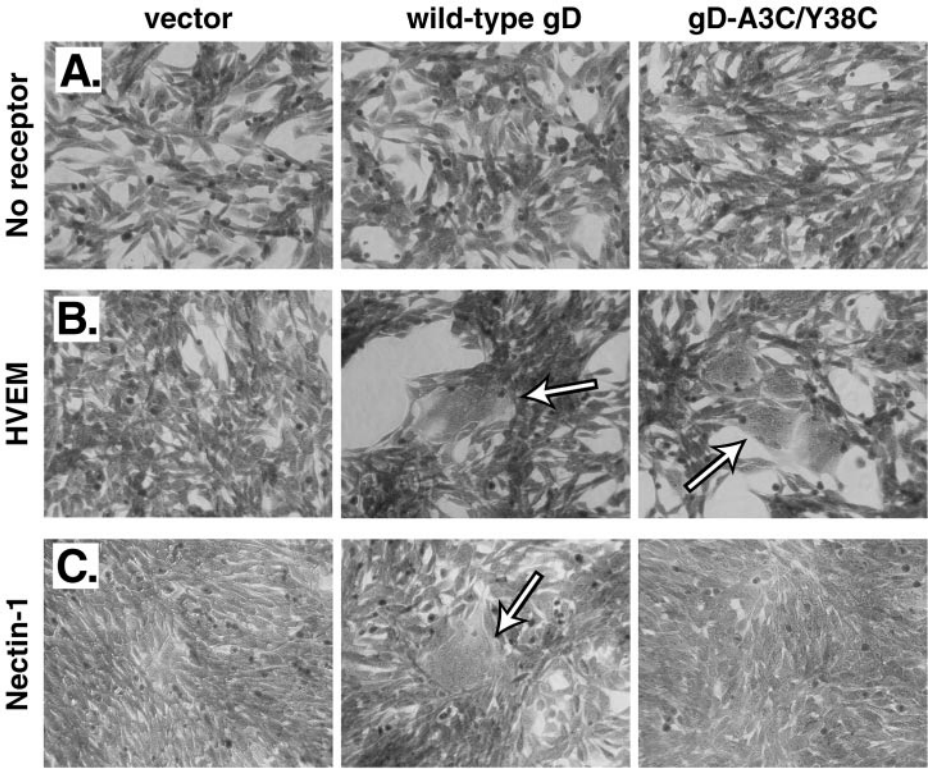

FIG. 2. Cell-cell fusion mediated by gD-A3C/Y38C. (A) Cells lacking a gD receptor (B78-H1) were transfected with plasmids encoding gB, gH, gL, and either wild-type gD, gD-A3C/Y38C, or vector DNA. Cells were stained, and syncytia (arrows) were viewed by microscopy. Representative images are shown. (B) Cells stably expressing HVEM (B78-H1-A10) were treated as above. (C) Cells stably expressing nectin-1 (B78-H1-C10) were treated as above.

of gD are unable to use mouse or human HVEM but can still use nectin-1 as a receptor. Thus, we considered it unlikely that any mutation upstream of residue 32 would disturb nectin-1 binding. However, gD-Y38 could be important for nectin-1 binding. Importantly, gD-Y38 is just downstream of the HVEM binding site (6) (Fig. 1C), and the observation that some MAbs block binding of nectin-1 and HVEM to gD makes it likely that the two binding sites overlap or are close together. Moreover, tyrosines often play a critical role in protein-protein interactions (2, 13). Furthermore, when one examines the structure of gD alone, Y38 is exposed on the surface (6), so this mutation is unlikely to have effects on the global structure of gD.

Consequently, we constructed gD molecules in which tyrosine 38 was mutated to cysteine, alanine, or phenylalanine (Fig. 3D). Neither gD-Y38C nor gD-Y38A bound nectin-1 (Fig. 3E), supporting our hypothesis that Y38 is essential for nectin-1 binding. Interestingly, gD-Y38F retained wild-type levels of nectin-1 binding, indicating that the phenyl ring rather than the terminal hydroxyl group of gD-Y38 plays an important role in the interaction.

Interestingly, gD-Y38C and gD-Y38F showed reduced binding to HVEM (approximately 50%), and gD-Y38A did not bind to this receptor at all (Fig. 3F). This suggests that although gD-Y38 does not contact HVEM (6), this residue may affect the structure of the N-terminal hairpin loop, and its mutation may compromise the HVEM binding site (Fig. 1C). In fact, in the gD-HVEM complex, gD-Y38 contacts several residues of the N-terminal gD hairpin loop (residues 1 to 6) (6). Moreover, this set of observations is evidence for overlap of the binding sites for HVEM and nectin-1 on gD. It is of interest that the double mutant gD-A3C/Y38C exhibited better binding to HVEM than the single mutant, gD-Y38C. We hypothesize that in the double mutant, a disulfide bond between cysteine 3 and cysteine 38 stabilizes the N-terminal loop and favors HVEM binding.

Selection of additional gD residues to analyze. In the structure of gD alone, the gD-Y38 side chain faces away from the core of gD and is fully accessible to solvent (Fig. 4A and B). We reasoned that gD-Y38 could play a key role in binding nectin-1, analogous to the role played by Y23 of HVEM in binding to gD (13). We hypothesized that other residues in this region would also have an effect on nectin-1 binding. For mutagenesis, we chose residues exposed on the gD surface near gD-Y38, i.e., R36, V37, H39, Q132, R134, P221, and F223 (Fig. 4C; Table 1). In addition, we focused on residues situated on the gD surface between gD-Y38 and the site of two MAb-resistant (*mar*) mutations, at T213 (T213M in the *mar* mutant of HSV-2 gD) (J. C. Whitbeck, Y. Zuo, et al., unpublished data) and S216 (S216N in the *mar* mutant of HSV-1 gD) (Fig. 4C) (42, 44, 46). These two residues lie on the same face of the molecule as gD-Y38, and the respective *mar* mutants are resistant to MAbs that inhibit nectin-1 binding (31, 44). Interestingly, Q132, which is adjacent to Y38, is also the site of a

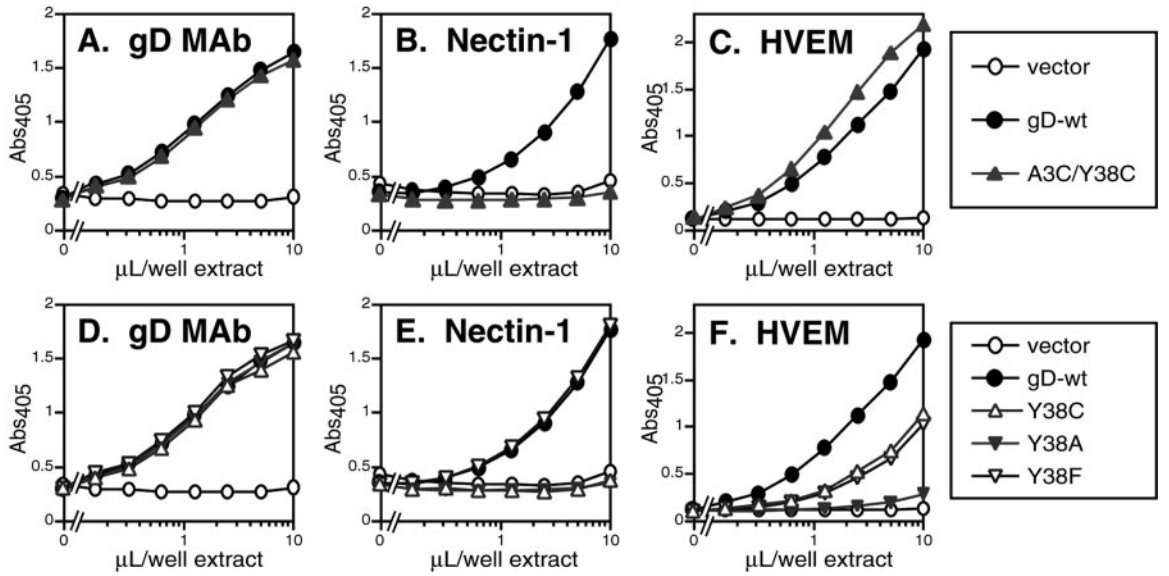

FIG. 3. Expression and receptor binding of gD-Y38 mutants. (A) gD quantitation by capture ELISA. Cell extracts were prepared from 293T cells transfected with plasmids encoding wild-type gD, gD-A3C/Y38C, or vector DNA. Dilutions of extracts were added to 96-well plates coated with the anti-gD MAb DL6. The amount of gD captured by the MAb was detected using anti-gD PAb. The cell extracts were then diluted in extraction buffer to obtain normalized levels of gD. Data are shown for normalized extracts. (B) Binding of gD-A3C/Y38C to nectin-1. Ninety-six-well plates were coated with the nectin-1 ectodomain (31), incubated with dilutions of transfected cell extracts normalized for gD content, and probed with an anti-gD PAb to detect the levels of gD binding. (C) Binding of gD-A3C/Y38C to HVEM. The 96-well plates were coated with the HVEM ectodomain (64) and treated as above. (D) gD quantitation by capture ELISA. Cell extracts were prepared and normalized as described for panel A. (E) Binding of gD-Y38 mutants to nectin-1. ELISA was performed as for panel B. (F) Binding of gD-Y38 mutants to HVEM. ELISA was performed as for panel C. Assays detecting gD binding to anti-gD MAb, nectin-1, and HVEM were run in parallel. In each case, data are shown for wild-type gD and three gD-Y38 mutants from one representative experiment.

mar mutation (26). The amino acids chosen for mutagenesis using this approach were T213 and S216, as well as D215, G218, L220, and R222. To determine the contribution of each of these residues to receptor interaction, we mutated each one to alanine (61) (Table 1). For controls, we included wild-type gD and two gD mutants, gD-Q27P and gD-D30A, that interact with nectin-1 but not HVEM (12, 15).

Receptor binding properties of the panel of gD mutants. Cells were transfected with plasmids encoding each mutant, cell extracts were normalized for gD content, and receptor binding was examined by ELISA using the appropriate extract dilutions. All of the mutants were tested concurrently, and data for three representative mutants are shown (Fig. 5A, B, and C). As expected from previous results (22, 31, 43), gD-Q27P (the rid1 mutant) bound better to nectin-1 than did wild-type gD (Fig. 5B) and failed to bind to HVEM (Fig. 5C). Among the new mutants, gD-D215A failed to bind nectin-1 and showed somewhat reduced binding to HVEM, while gD-L220A showed markedly reduced binding to nectin-1 and wild-type levels of HVEM binding.

To compare all of the mutants, we expressed the data for each mutant as a percentage of wild-type gD binding, using a single concentration of gD (5 μl/well extract) (Fig. 5D and E). As expected, wild-type gD bound both receptors, gD-D30A bound nectin-1 but not HVEM, and gD-Q27P failed to bind HVEM but showed increased binding to nectin-1.

The new gD mutants were divided into categories based on their level of binding to nectin-1 and their ability to mediate fusion of nectin-1-bearing cells (see below). Seven mutants bound to nectin-1 at levels that were at least 25% that of wild-type gD (Fig. 5D, category 1). Four mutants (R36A, H39A, G218A, and L220A) bound nectin-1 at levels that were detectable but less than 25% of wild-type gD (category 2). The remaining six mutants (R134A, D215A, P221A, Y38A, Y38C, and A3C/Y38C) showed no detectable binding to nectin-1 (categories 3 and 4), indicating that the nectin-1 binding site may include some or all of these mutated residues.

In contrast, all but three of the gD mutants bound HVEM at levels that were at least 25% that of wild type (Fig. 5E). The three mutants that did not bind HVEM or bound poorly were gD-R36A, gD-V37A, and gD-Y38A. Although none of these residues contact HVEM, they may affect HVEM binding by altering the conformation of the N-terminal loop of gD (6, 12). Overall, our results identified eight amino acids that may be part of a nectin-1 binding site, including six residues that do not participate in HVEM binding. Whereas all of the gD mutants except Y38A bound at least one receptor, none bound to nectin-2 (data not shown).

Ability of the gD mutants to mediate cell-cell fusion. Previous studies showed that some gD mutants that lack demonstrable binding to receptors can still function in cell-cell fusion and virus entry (12, 14, 27, 31, 38, 40, 51, 60). This difference is likely based on affinity, i.e., the binding of mutants with very low affinity for receptor is not detected by stringent binding assays but is still sufficient for entry, especially in an excess of receptor.

We tested gD function in a luciferase-based quantitative cell-cell fusion assay (3, 12, 41, 49, 51). In this assay, effector

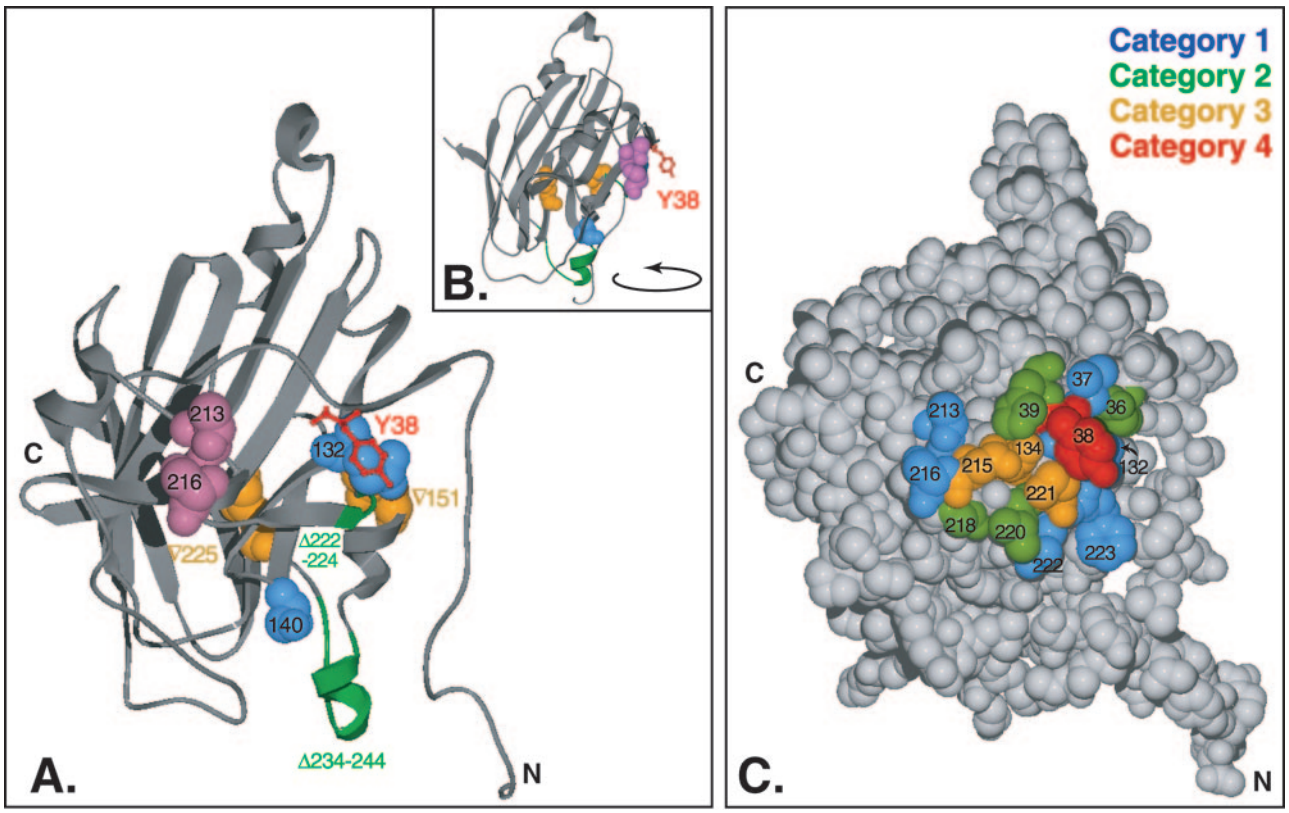

FIG. 4. Potential nectin-1 binding site on gD. (A) Supporting evidence for the location of the face of nectin-1 binding on gD. The location of gD-Y38 (red) is indicated. The sites of MAb-resistant (*mar*) mutations for MAbs belonging to group Ia (213 and 216 [pink]) or group Ib (132 and 140 [blue]) are shown (42, 44, 46; Whitbeck, et al., unpublished). Group Ia MAbs block nectin-1 binding, while group Ib MAbs block both nectin-1 and HVEM binding (31, 47). Deletion of residues 222 to 224 (green) or 234 to 244 (green) results in a loss of gD interaction with both nectin-1 and HVEM (7, 29, 63). gD carrying insertion mutations at residue 151 (yellow) or 225 (yellow) also fails to interact with nectin-1 or HVEM (7, 29, 69). (B) The molecule from panel A has been rotated around the *y* axis to demonstrate the accessibility of gD-Y38 (red). (C) Contribution of gD residues to nectin-1 interaction. gD is shown in the same orientation as in panel A but in a space-filling format, such that only the surface of gD is visible. Residues that were replaced with alanine in this study are colored according to category (Table 1). The N and C termini of gD are indicated. Mutation of category 1 residues (blue; V37, Q132, T213, S216, R222, or F223) had no significant effect on the nectin-1 interaction. Mutation of category 2 residues (green; R36, H39, G218, or L220) resulted in a decreased nectin-1 binding and retention of the ability to fuse nectin-1-bearing cells. Mutation of category 3 residues (orange; R134, D215, or P221) resulted in a loss of detectable nectin-1 binding but retention of the ability to fuse nectin-1-bearing cells. Mutation of the category 4 residue (red; Y38) resulted in a loss of nectin-1 binding and fusion of nectin-1-bearing cells.

cells are prepared by transfecting CHO-K1 cells in a 96-well plate with plasmids encoding T7 RNA polymerase, gB, gH, gL, and one of the gD mutants. Target cells are prepared by transfecting cells that stably express HVEM (CHO-HVEM12) or nectin-1 (CHO-R3A) with a plasmid encoding the luciferase gene under control of the T7 promoter. Target and effector cells were mixed, incubated, and assayed for luciferase activity as a measure of cell-cell fusion. This assay was chosen so that we could compare the effect of each mutation on the extent of fusion in a single quantitative experiment.

One 96-well plate of effector cells was used in the fusion assay, and a duplicate plate was fixed with PFA to determine the amount of gD by CELISA using PAb to gD. All of the gD mutants were expressed at similar levels (Fig. 6A), suggesting they were folded properly enough to be transported to the plasma membrane. In the fusion assay, the three control gD molecules behaved as expected, i.e., effector cells expressing wild-type gD fused with target cells bearing either receptor, while cells expressing gD-Q27P or gD-D30A fused only with nectin-1-bearing target cells (Fig. 6B and C). All of the gD mutants that bound nectin-1 were able to mediate fusion with nectin-1-bearing target cells (Fig. 6B; Table 1, categories 1 and 2). This included R36A, H39A, G218A, and L220A, all of which showed markedly reduced binding to nectin-1 (Fig. 5D). Moreover, three mutants (R134A, D215A, and P221A) that did not detectably bind to nectin-1 still mediated fusion with nectin-1-bearing cells (category 3). Thus, the detrimental effect of mutations from categories 2 and 3 was more apparent in the binding assay than in the fusion assay.

Only three gD mutants (Y38A, Y38C, and A3C/Y38C) failed to mediate fusion with nectin-1-bearing cells (category 4). All of these mutants fail to bind nectin-1 (Fig. 5D) and carry a mutation at position 38, indicating the importance of this residue. Furthermore, mutation of residues adjacent to this residue (R36, H39, P221) in the three-dimensional (3-D) structure (Fig. 4C) had major effects on binding to nectin-1, though fusion of nectin-1-bearing cells was not affected.

The only mutant in this study that could neither bind HVEM (Fig. 5E) nor mediate fusion of HVEM-bearing cells was gD-R36A (Fig. 6C). Since this mutant was able to mediate fusion

TABLE 1. Categorization of the gD mutant proteins

gD mutation	Ability of gD mutant to mediate process via specific receptor				Category[e]
	Nectin-1		HVEM		
	Binding	Fusion	Binding	Fusion	
V37A	+	+	↓	+	1
Y38F	+	+	+	+	1
Q132A	+	+	+	+	1
T213A	+	+	+	+	1
S216A	+	+	+	+	1
R222A	+	+	+	+	1
F223A	+	+	+	+	1
R36A	↓	+	−	−	2
H39A	↓	+	+	+	2
G218A	↓	+	+	+	2
L220A	↓	+	+	+	2
R134A	−	+	+	+	3
D215A	−	+	+	+	3
P221A	−	+	+	+	3
Y38A	−	−	−	+	4
Y38C	−	−	+	+	4
A3C/Y38C	−	−	+	+	4
Wild-type gD	+	+	+	+	Control[a]
D30A[b]	+	+	−	−	Control
Q27P[c]	+++[d]	+	−	−	Control

[a] Results for these control gD proteins are included for comparison.
[b] The D30A mutation was previously described by Connolly et al. (12).
[c] The Q27P mutation was originally identified by Dean et al. (15).
[d] +++, binding is increased compared to that of wild-type gD.
[e] Category 1 mutants bind nectin-1 and mediate fusion of nectin-1-bearing cells. Category 2 mutants have reduced nectin-1 binding and mediate fusion of nectin-1-bearing cells. Category 3 mutants have undetectable nectin-1 but mediate fusion of nectin-1-bearing cells. Category 4 mutants fail to bind nectin-1 or mediate fusion of nectin-1-bearing cells.

of target cells bearing nectin-1 (Fig. 6B) but not those bearing nectin-2 (data not shown), its phenotype is distinct from that of gD-Q27P (rid1), which uses nectin-1 and nectin-2 but not HVEM as a receptor (Table 1). Among the gD mutants examined in this study, gD-Q27P was the only one that mediated fusion with target cells bearing nectin-2 (data not shown). The fact that all of the mutants mediated fusion of at least one of the target cell lines suggests that none were globally affected in structure by the mutation. Immunologic evidence to support this conclusion is presented in a later section.

Does gD-A3C/Y38C mediate HSV entry into cells bearing human HVEM or nectin-1? Although it has been known for some time that the rid1 virus uses nectin-1 but not HVEM as a receptor, no HSV strain that uses HVEM but not nectin-1 has yet been isolated. The properties of gD-A3C/Y38C suggest that a virus bearing this protein in its envelope would have such a phenotype. To test this idea, we examined gD-A3C/Y38C in a complementation assay (7, 12, 34, 46).

L cells were transfected with a plasmid encoding wild-type gD, gD-A3C/Y38C, or gD-Q27P and then infected with a gD-null HSV complemented with wild-type gD. The progeny would be genotypically gD-null but would carry either wild-type or mutant gD in its envelope. Expression of gD on the cell surfaces was confirmed by CELISA (data not shown). We tested the ability of the complemented viruses to enter CHO-HVEM (M1A) or CHO-nectin-1 (M3A) cells that carry the *lacZ* gene under the control of the HSV ICP4 promoter. Entry was measured by assaying for β-galactosidase activity (32, 43, 57). Virus complemented with wild-type gD infected both cell types, while virus complemented with gD-Q27P (rid1) infected only nectin-1-bearing cells (Fig. 7). In agreement with the fusion assays, virus complemented with gD-A3C/Y38C entered HVEM-bearing cells but not nectin-1-bearing cells. In fact, this mutant had nearly the same complementation activity as wild type on HVEM-bearing cells. Construction of a recombinant virus carrying these gD mutations is in progress.

Structural integrity of gD mutant proteins. Since all of the gD mutants functioned with at least one receptor, we believe that the mutations had no major effect on gD structure. To confirm this, we screened extracts of 293T cells transfected with each mutant by using anti-gD MAbs that recognize different antigenic sites (Table 2). All of the gD mutants bound PAb R7 and two MAbs (DL6 and 1D3) that recognize linear epitopes (7, 10, 19). All of the mutant proteins also bound MAbs HD1 and DL2, which recognize different discontinuous epitopes (11, 44, 45, 50). This suggests that the mutations did not have global effects on gD structure.

Interestingly, nine mutants failed to bind DL11, a group Ib MAb that recognizes a discontinuous epitope, blocks gD binding to both HVEM and nectin-1, and efficiently neutralizes virus entry (Table 2; Fig. 8A). Since all of the residues identified by DL11 reactivity loss are in proximity to each other in the 3-D structure and all are on the surface of gD, we believe they may constitute at least part of the DL11 epitope.

Four gD mutants failed to bind to AP7, a neutralizing MAb that recognizes a discontinuous epitope that is affected by mutation of residues at the N terminus or insertions or truncation of amino acids at the C terminus of the gD ectodomain (Table 2) (5, 7, 42, 48). The loss of AP7 reactivity with gD-Q27P and gD-D30A agreed with previous reports (12, 15, 42). The failure of gD-R36A and gD-F223A to bind AP7 was unexpected and suggests that these residues are either within the AP7 epitope or influence its conformation. Since the 3-D structure of gD excludes the last 50 amino acids of the C terminus of the ectodomain, further information about where this antibody binds can only be undertaken when a more complete gD structure becomes available.

DISCUSSION

Comparison of crystal structures of gD alone and gD bound to HVEM reveal that the N terminus of gD undergoes a conformational change when it binds HVEM, such that it forms a hairpin loop that contacts CRD1 and CRD2 of the receptor (6). Here, we attempted to lock the N terminus of gD in a looped conformation by inserting cysteine residues at positions 3 and 38, which are predicted to be within the atomic distance of a disulfide bond. We speculated that normally there is an equilibrium between the looped and unlooped forms of the N terminus in unliganded gD and that substitution of A3 and Y38 with cysteines could stabilize the looped form (17). Biochemical and structural studies using purified gD-A3C/Y38C protein are in progress to confirm that this disulfide bond does indeed form. It is unlikely that these mutations

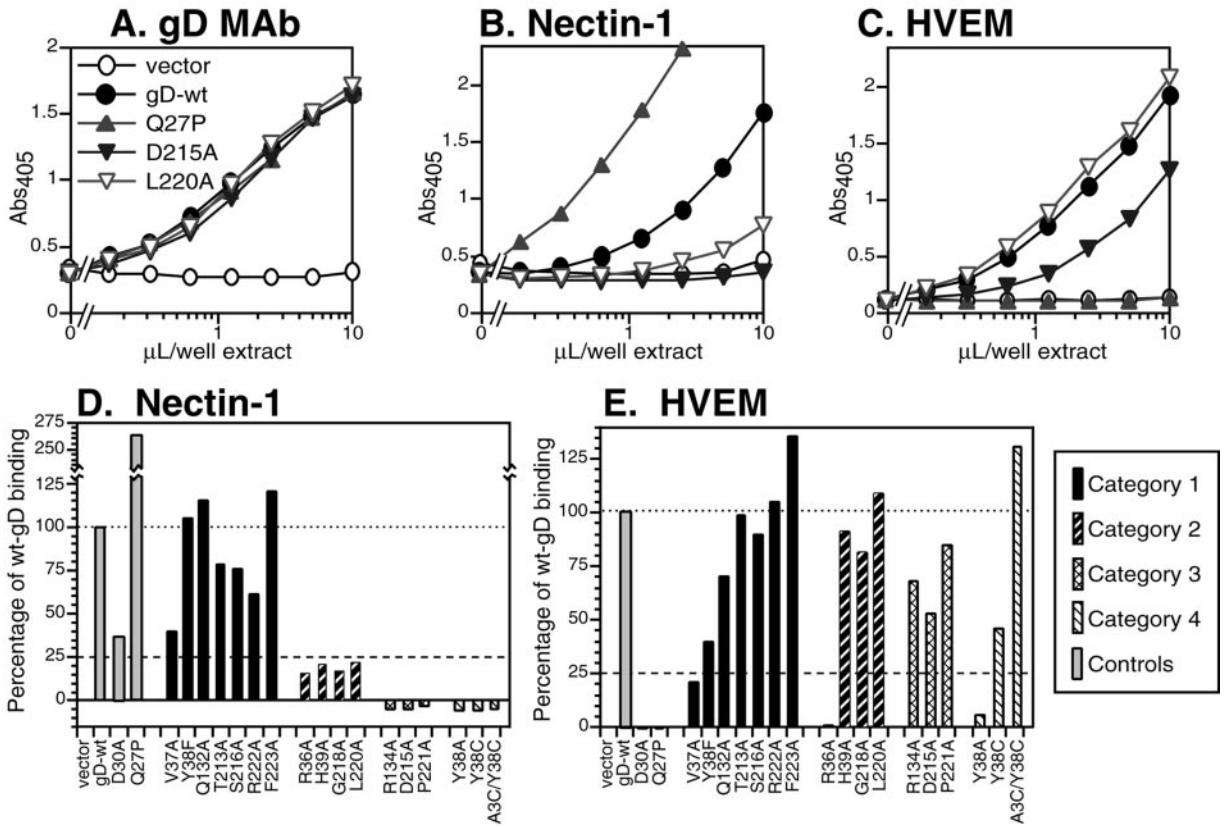

FIG. 5. Expression and receptor binding of gD mutants. (A) gD quantitation by capture ELISA. ELISA was performed as for Fig. 3A. Data are shown for normalized extracts of wild-type gD and three gD mutants. (B) Binding of gD mutants to nectin-1. ELISA was performed as for Fig. 3B. (C) Binding of gD mutants to HVEM. ELISA was performed as for Fig. 3C. Assays detecting gD binding to HVEM, nectin-1, and anti-gD MAbs were run in parallel. (D) Nectin-1 binding for a panel of the gD mutants. Binding data for a single dilution of normalized extract (5 μl/well) are plotted. The negative control (vector) signal was subtracted, and receptor binding is expressed as a percentage of wild-type gD receptor binding. Results obtained with wild-type gD and two known gD mutants (D30A and Q27P) are shown for comparison (gray bars) (12, 43, 64). For clarity, the *y* axis is broken at 125%. The gD mutants are divided into four categories based on the overall phenotype exhibited for interactions with nectin-1 (Table 1). Category 1 mutants (black) have near-wild-type levels (≥25%) of binding to nectin-1. Category 2 mutants (heavy stripes) have impaired binding to nectin-1 (<25% of wild type). Category 3 (cross-hatched) and category 4 (light stripes) mutants do not bind nectin-1 at detectable levels. (E) HVEM binding for a panel of gD mutants. Binding data for a single dilution of normalized extract (5 μl/well) are plotted as described above, and the mutants are divided by category (Table 1).

caused aberrant disulfide bonding, since the protein retained most of its antigenic structure.

Assuming the gD-A3C/Y38C N terminus adopts the same looped conformation as that of gD bound to HVEM, creation of this loop in the absence of HVEM is insufficient to trigger the fusion machinery in a cell-cell fusion assay (Fig. 2). Thus, additional conformational changes in gD may be required to trigger fusion, possibly in residues downstream of amino acid 259 that were absent in the crystal structures. Indeed, we recently showed that some of these residues that were previously defined as comprising a functional region (FR) called FR4 (7) form a "profusion domain" that is separate and distinct from the portions of gD that contact HVEM or nectin-1 (9). We consider it unlikely that the absence of a gD receptor on the target cells in the syncytium formation assay affected fusion efficiency simply by lowering the levels of cell-cell binding, since initial binding to heparan sulfate proteoglycans could still be mediated by gB (66).

gD-Y38 is a critical residue for nectin-1 binding. Unexpectedly, gD-A3C/Y38C lost the ability to interact with nectin-1 (Fig. 2C, 3B, and 6B). Two possible explanations are that (i) the locked N-terminal loop occludes the nectin-1 binding site, or (ii) one or both of the residues that were mutated are critical in themselves for nectin-1 binding. To address these possibilities, we examined the properties of the single mutants gD-Y38C, gD-Y38A, and gD-Y38F. Neither of the first two mutants was able to bind nectin-1, showing that gD-Y38 is a critical residue for nectin-1 binding. Interestingly, gD-Y38F bound nectin-1 as well as wild-type gD, showing that the phenyl ring, rather than the hydroxyl group, of tyrosine forms the critical contacts with this receptor (Fig. 3E and 6B). Another interesting observation was that gD-Y38A was unable to bind to either receptor, although it was still functional in fusion assays employing HVEM as a receptor (Fig. 3 and 6). With the exception of MAb DL11, all of the other MAbs bound to gD-Y38A, indicating no global change in structure. Although gD-Y38 is not a contact residue for HVEM, it is adjacent to the HVEM binding site (Fig. 8B and C) and appears to be important for HVEM binding, which may account in part for the

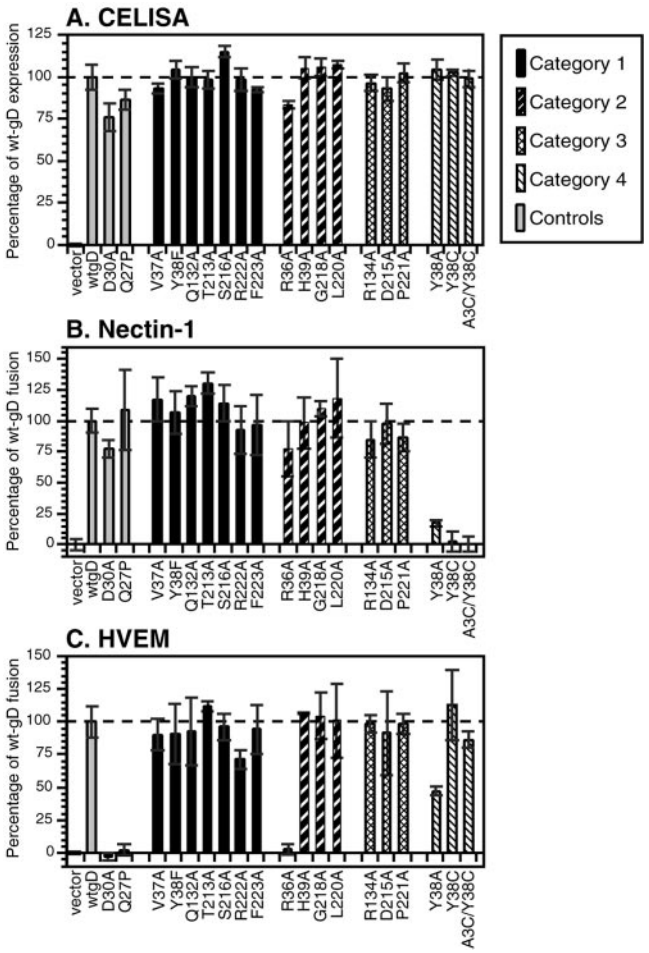

FIG. 6. Cell-cell fusion mediated by gD mutants. (A) Cell surface expression of gD mutants based on CELISA results. CHO-K1 cells transfected with plasmids encoding gB, gH, gL, a gD mutant, and T7 polymerase were seeded on 96-well plates, and expression of gD on the cell surface was detected using dilutions of anti-gD PAb. (B) Nectin-1-mediated fusion. CHO-K1 cells stably expressing nectin-1 (CHO-R3A) were transfected with a plasmid encoding the luciferase gene under the control of the T7 promoter and cocultivated with the cells described for panel A. The cells were lysed and assayed for luciferase activity as a measure of cell-cell fusion. The mean values and standard deviations from triplicate wells of one experiment are shown. Results obtained with wild-type gD and two known gD mutants (D30A and Q27P) are shown for comparison (gray bars). The gD mutants are divided into four categories based on the overall phenotypes exhibited for interactions with nectin-1 (Table 1). Category 4 gD mutants (light stripes) failed to mediate fusion with cells expressing nectin-1. The rest of the mutants mediated near-wild-type levels of fusion. (C) HVEM-mediated fusion. CHO-K1 cells stably expressing HVEM (CHO-HVEM12) were treated as for panel B.

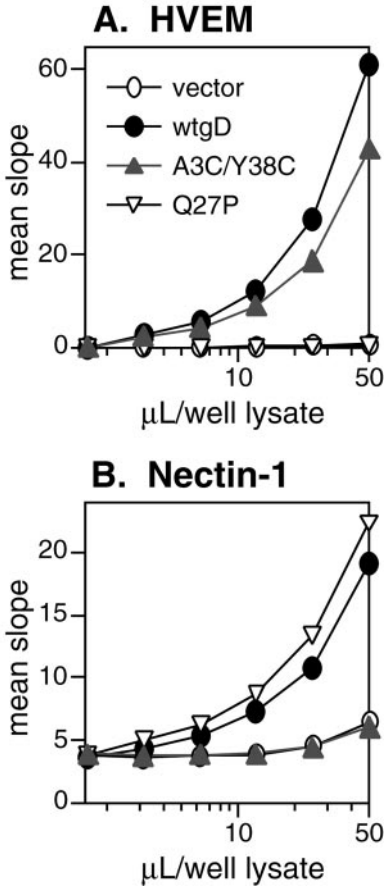

FIG. 7. gD-A3C/Y38C mediates HSV entry into cells. L cells were transfected with plasmids encoding gD mutants or empty vector, incubated overnight, and infected with gD-null HSV that had been phenotypically complemented with wild-type gD to allow for entry. Cell lysates containing progeny virions complemented with the gD mutants were harvested and assayed for entry activity. CHO-K1 cells that carry *lacZ* under control of the ICP4 promoter and express HVEM (M1A) or nectin-1 (M3A) were incubated overnight with dilutions of complemented cell lysates. β-Galactosidase production was used as a measure of virus entry. Data are shown for wild-type gD and two gD mutants. (A) Entry into cells expressing HVEM; (B) entry into cells expressing nectin-1.

overlapping nature of these receptor binding sites that had been noted in previous studies (22, 31, 47).

gD-Y38 also lies within FR1 and in close proximity to FR2 and FR3 of gD (7). These FRs are linear stretches in gD that were defined by mutations that prevent entry into cells. The Vero-derived VD60 cells (34) used to define these FRs express functional homologs of both nectin-1 and HVEM (41); thus, we and others expected the nectin-1 binding site to map near these regions. Fittingly, insertion mutations at residue 151 (FR2), directly adjacent to Y38, or a deletion of residues 222 to 224 or 234 to 244 (in FR3) prevent nectin-1 and HVEM binding (Fig. 4A) (29, 62, 69). Moreover, mutations that confer resistance to neutralization by anti-gD MAbs known to block entry via nectin-1 (*mar* mutations) occur on the same face of the molecule as gD-Y38 (44, 46; Whitbeck et al., unpublished), suggesting that this is the face to which nectin-1 binds.

HVEM mutagenesis demonstrated that Y23 of HVEM is a contact residue that serves as a hot spot for gD binding (13), a feature common to tyrosine residues that occur at protein-protein interfaces (2). gD-Y38 may serve as an analogous hot spot on gD for nectin-1 binding. Importantly, the gD-Y38 side chain faces away from the core of gD, is fully accessible to solvent, and is therefore readily available to bind nectin-1 (Fig. 4B).

Mapping the nectin-1 binding site on gD. HVEM-Y23 is located at the center of the HVEM-gD interface (6), and

TABLE 2. MAb reactivity of the gD mutant proteins

gD mutation	MAb reactivity						PAb reactivity (R7)	Category
	Linear epitopes		Discontinuous epitopes					
	DL6 (IIb)[a]	1D3 (VII)	DL2 (VI)	HD1 (Ia)	DL11 (Ib)	AP7 (XII)		
V37A	+	+	+	+	+	+	+	1
Y38F	+	+	+	+	+	+	+	1
Q132A	+	+	+	+	+	+	+	1
T213A	+	+	+	+	+	+	+	1
S216A	+	+	+	+	+	+	+	1
R222A	+	+	+	+	−	+	+	1
F223A	+	+	+	+	+	−	+	1
R36A	+	+	+	+	−	−	+	2
H39A	+	+	+	+	−	+	+	2
G218A	+	+	+	+	+	+	+	2
L220A	+	+	+	+	−	+	+	2
R134A	+	+	+	+	−	+	+	3
D215A	+	+	+	+	−	+	+	3
P221A	+	+	+	+	+	+	+	3
Y38A	+	+	+	+	−	+	+	4
Y38C	+	+	+	+	−	+	+	4
A3C/Y38C	+	+	+	+	−	+	+	4
Wild-type gD	+	+	+	+	+	+	+	Control
D30A	+	+	+	+	+	−	+	Control
Q27P	+	+	+	+	+	−	+	Control

[a] Roman numerals denote the epitope group to which each MAb belongs.

residues around this site contribute to gD binding as well (13). By analogy, if gD-Y38 represents a hot spot for nectin-1 binding, we hypothesized that some of the residues that surround it and others on the same face as Y38 would also contribute to nectin-1 binding. Therefore, we mutated residues adjacent to gD-Y38, residues that are sites of known *mar* mutations, and residues that span the surface of gD between these two sites (Fig. 4C) (26, 42, 44; Whitbeck et al., unpublished). The phenotypes of these mutants fell into four categories in terms of nectin-1 binding and cell-cell fusion (Table 1).

Category 1. Many of the mutations did not disrupt nectin-1 binding (category 1), indicating that these residues do not contribute individually to nectin-1 binding. However, we cannot rule out the possibility that these are contact residues for nectin-1, since previous studies showed that mutation of the majority of residues at the gD-HVEM interface have little or no effect on receptor binding or function (12, 13). Interestingly, mutating the *mar* mutant residues to alanine (gD-Q132, gD-T213, and gD-S216) did not affect nectin-1 binding.

Category 2. Four of the mutations exhibited a marked reduction in nectin-1 binding but no effect on cell-cell fusion of nectin-1-bearing cells. Based on the binding data, we argue that these residues contribute to nectin-1 binding, and their phenotype is similar to that of many mutants at the gD-HVEM interface (12, 13). Due to the inward orientation of the gD-R36 side chain, mutation of this residue may disrupt local gD structure, and this may account for the effects seen for HVEM and nectin-1 binding. Mutation of this residue and gD-H39, which

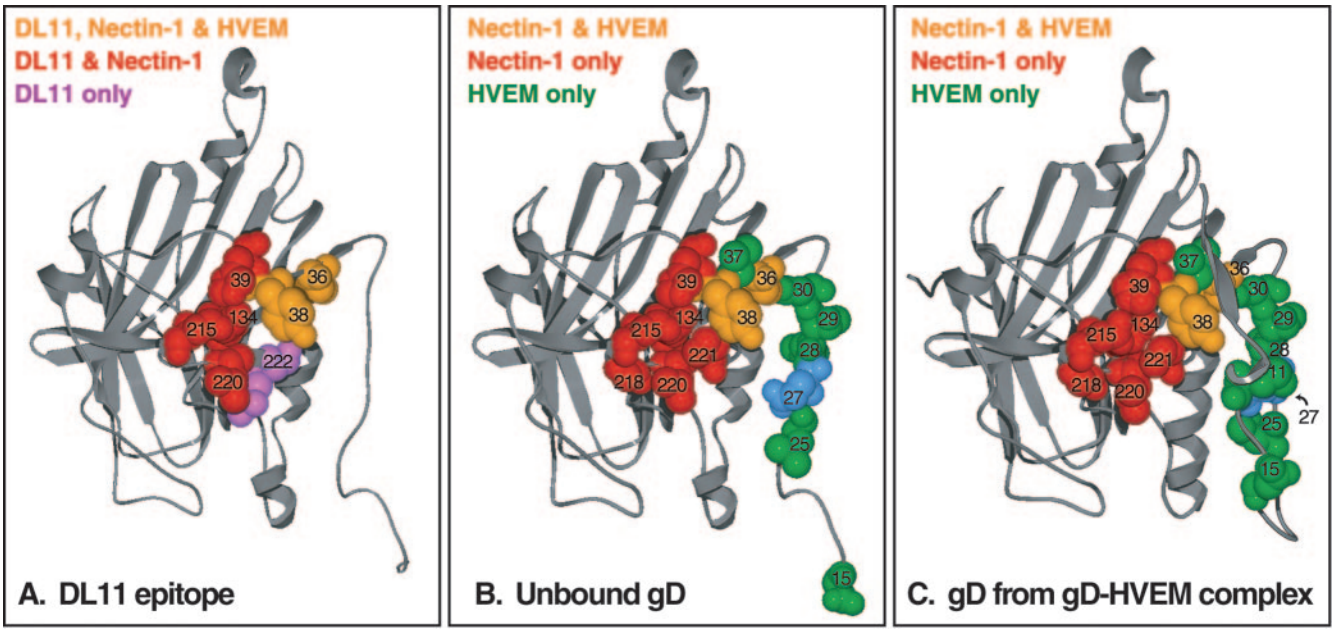

FIG. 8. The DL11, nectin-1, and HVEM binding sites on gD are distinct but overlapping. (A) Mapping the DL11 epitope. The residues that contributed to DL11 binding in this study (Table 2) are colored and shown in space-filling format on the structure of unliganded gD. The color of each residue corresponds to its contribution to nectin-1 and HVEM binding. Yellow residues contribute to DL11, nectin-1, and HVEM binding, while red residues contribute to only DL11 and nectin-1 binding. The purple residue affects DL11 binding, but not that of nectin-1 or HVEM. (B) Crystal structure of unliganded gD. Using results from this study and a previous mutagenesis study (12), residues that contribute to nectin-1 or HVEM binding are shown in space-filling format. Yellow residues contribute to both nectin-1 and HVEM binding, while red residues contribute to only nectin-1 binding and green residues contribute to only HVEM binding. Mutation of the blue residue, gD-Q27, results in increased nectin-1 binding and a loss of HVEM binding. (C) Crystal structure of gD from the gD-HVEM complex. Residues that contribute to HVEM and nectin-1 binding are colored as for panel B. For clarity, the HVEM molecule is not shown (Fig. 1C).

is adjacent to gD-Y38, may affect nectin-1 binding by altering the orientation of the gD-Y38 side chain. In contrast, gD-G218 and gD-L220 are more distant from Y38 but are also in category 2. The position of these residues is consistent with the notion that hot spot residues are often surrounded by a ring of energetically less important contact residues whose primary role is to exclude solvent from the interface (2, 8).

Categories 3 and 4. All mutants that failed bind to nectin-1 and mediate fusion of cells expressing nectin-1 (category 4) contained a mutation of gD-Y38, highlighting its central role in nectin-1 binding.

Three of the mutants failed to bind nectin-1 at detectable levels but retained the ability to fuse nectin-1-bearing cells (category 3). Again, this phenotype was seen for several contact residues between gD and HVEM (12, 13). In fact, fusion and entry in the absence of appreciable receptor binding has been previously shown for HSV strains using nectin-2 (38, 51, 60) and has been attributed to the higher sensitivity of entry and fusion assays for picking up low-affinity interactions. Thus, a wide range of affinities between gD and nectin-1 is tolerated for the entry of HSV, pseudorabies virus, and bovine herpes virus (14, 31, 40).

Interestingly, all residues defined by category 3 mutations cluster at the center of the proposed nectin-1 binding site, adjacent to gD-Y38 (Fig. 4C). A structure of the nectin-1-gD complex will be required to substantiate this as the site of nectin-1 binding. Mutation of these residues may disrupt nectin-1 binding by eliminating direct contacts with nectin-1 or by altering the contacts between gD-Y38 and nectin-1. For example, the guanidinium of the gD-R134 side chain forms a hydrogen bond with the carbonyl oxygen of gD-Y38, and disruption of this interaction may alter the position of gD-Y38. Likewise, gD-D215 contacts gD-H95, which is very close to gD-Y38, and thus mutation of gD-D215 may affect gD-Y38 indirectly. The final member of this category is gD-P221, and mutation of this proline could cause local structural differences that disrupt nectin-1 binding.

HVEM and nectin-1 binding sites are distinct but overlapping. The majority of the mutants showed wild-type levels of HVEM binding and fusion of HVEM-bearing cells, reinforcing the notion that nectin-1 and HVEM bind to distinct sites on gD. However, gD-R36A, gD-V37A, and gD-Y38A displayed markedly reduced HVEM binding, and gD-R36A was unable to mediate fusion via HVEM. Interestingly, none of these residues are contact residues for HVEM, emphasizing that mutants that are defective in binding or function do not necessarily carry mutations in contact residues. The properties of these mutants are evidence that the sites on gD for the two receptors contain both distinct and overlapping regions. Previous work showed that soluble forms of either receptor blocked HSV entry via both homologous and heterologous receptors (22).

It is noteworthy that with HVEM bound to gD, nectin-1 would have no access to gD-Y38 (Fig. 8C). In fact, the gD N terminus may adopt at least three different conformations: an extended conformation when in the unbound form, a looped conformation when bound to HVEM, and an unknown conformation when bound to nectin-1, perhaps a conformation closer to that of the unbound form.

TABLE 3. Panel of gD mutants with altered receptor usage

gD mutant	Ability to mediate fusion of cells bearing:		
	HVEM	Nectin-1	Nectin-2
Wild-type gD	+	+	−
gD-A3C/Y38C[a]	+	−	−
gD-Y38A[a]			
gD-T29A[b]	−	+	−
gD-D30A[b]			
gD-R36A[a]			
gD-Q27P[c]	−	+	+
gD-L25P[d]	+	+	+
gD-L28A[b]			

[a] Mutant generated and characterized in this study.
[b] Connolly et al. (12).
[c] Warner et al. (60) and Geraghty et al. (22).
[d] Lopez et al. (36) and Yoon et al. (68).

Epitope mapping of MAbs DL11 and AP7. The panel of gD mutants provided important information about the epitopes for MAbs DL11 (group Ib) and AP7 (group XII) (45). It is worth noting that DL11 is one of the most potent neutralizing MAbs to HSV that we have in our collection (16, 46). This antibody blocks binding of both HVEM and nectin-1 to virion gD (31, 47). Importantly, all mutants of Y38 were DL11 negative but positive for all of other conformation-dependent antibodies (Fig. 8A; Table 2). Other mutants that failed to bind to this important antibody included R36, H39, R134, and D215. Most of the residues that contributed to DL11 binding also contributed to nectin-1 binding. In fact, two residues that contributed to the DL11 epitope affected both nectin-1 and HVEM binding (Fig. 8A). Thus, the DL11 epitope partially overlaps both the nectin-1 and HVEM binding sites, which explains why DL11 is able to block interaction with both receptors. In addition, one residue that contributes to DL11 binding does not contribute to either the nectin-1 or HVEM interactions (Fig. 8A). This indicates that the DL11 epitope is distinct from both the HVEM and nectin-1 binding sites.

MAb AP7 is important because residues at both the N and C termini of the gD ectodomain affect the AP7 epitope (7). This suggests that these two regions are near each other in the 3-D structure or that they contribute indirectly to the formation of the AP7 binding epitope. Since the C terminus of the gD ectodomain was disordered in the structure, we do not yet know whether the N and C termini of native gD make contact. Interestingly, although the C terminus is not required for receptor binding, truncation of this region increases the affinity of gD for both nectin-1 and HVEM (32, 65). Earlier studies showed that gD-L25, gD-Q27, and gD-D30 are important for AP7 binding (12, 15, 42). Here, we found that gD-R36 is also critical. We hypothesize that these four amino acids constitute part of the AP7 epitope. gD-F223 within the α3 α-helix is also important for AP7 binding and coincidentally contacts Q27. It is therefore possible that gD-F223 stabilizes the AP7 epitope through this contact or that gD-F223 participates in formation of the AP7 epitope.

gD mutants with alterations in receptor usage. Finally, this study generated gD mutants that exhibited altered receptor

usage. The combination of these mutants with previously characterized mutants completes a panel (Table 3) that may be useful in dissecting the roles played by the various HSV receptors during in vitro and in vivo infections. The panel includes mutants that can use HVEM only, nectin-1 only, both nectin-1 and nectin-2, or all three receptors. gD-A3C/Y38C is the most valuable member of this panel because it is, to our knowledge, the first mutant identified that mimics wild-type gD for HVEM interaction but fails to bind nectin-1 or use this receptor in cell-cell fusion and virus complementation assays. Efforts are now under way to recombine this and other interesting gD mutants into the wild-type KOS virus background for pathogenesis studies. We hypothesize that a virus containing the gene for gD-A3C/Y38C should have this same unique receptor usage phenotype. Using recombinant viruses, we hope to confirm that the mutants retain no unexpected residual levels of receptor usage and verify the DL11 MAb binding results by testing for DL11 neutralization of these viruses.

Which receptors are used during HSV infection in vivo is not known. Some have proposed that nectin-1 represents the principal receptor for HSV in vivo due its expression on neurons (4, 69); however, nectin-1 localizes to cell junctions and may not be accessible to extracellular virus (56, 67). All of the HSV primary isolates that have been tested can use both HVEM and nectin-1 for entry (30). Furthermore, gD has the same affinity and similar binding kinetics for both HVEM and nectin-1 (32, 65). Quantitation of receptor levels on susceptible cell types indicated that both receptors are highly efficient, even at low levels of expression (30). This suggests that receptor usage in vivo may be determined by the availability of receptors on a particular cell type or tissue. Using mutants from this panel for in vivo experiments may illustrate the relative importance of each receptor.

ACKNOWLEDGMENTS

We thank N. W. Fraser, D. C. Johnson, and P. G. Spear for reagents and I. Baribaud, T. M. Cairns, C. Krummenacher, and R. S. B. Milne for valuable advice.

This investigation was supported by Public Health Service grant AI-18289 to G.H.C. and R.J.E. and by grant AI-056045 from the National Institute of Allergy and Infectious Diseases and grant NS-36731 from the National Institute of Neurologic Diseases and Stroke to R.J.E. and G.H.C.

ADDENDUM IN PROOF

Additional mutations to gD were reported by Manoj et al. (S. Manoj, C. R. Jogger, D. Myscofski, M. Yoon, and P. G. Spear, Proc. Natl. Acad. Sci. USA **101:**12414–12421, 2004). Our predicted location for the nectin-1 binding site on gD is consistent with results from that study.

REFERENCES

1. **Binley, J. M., R. W. Sanders, B. Clas, N. Schuelke, A. Master, Y. Guo, F. Kajumo, D. J. Anselma, P. J. Maddon, W. C. Olson, and J. P. Moore.** 2000. A recombinant human immunodeficiency virus type 1 envelope glycoprotein complex stabilized by an intermolecular disulfide bond between the gp120 and gp41 subunits is an antigenic mimic of the trimeric virion-associated structure. J. Virol. Methods **74:**627–643.
2. **Bogan, A. A., and K. S. Thorn.** 1998. Anatomy of hot spots in protein interfaces. J. Mol. Biol. **280:**1–9.
3. **Cairns, T., R. S. B. Milne, M. Ponce de Leon, D. K. Tobin, G. H. Cohen, and R. J. Eisenberg.** 2003. Structure-function analysis of herpes simplex virus gD and gH/gL: clues from gD/gH chimeras. J. Virol. **77:**6731–6742.
4. **Campadelli-Fiume, G., F. Cocchi, L. Menotti, and M. Lopez.** 2000. The novel receptors that mediate the entry of herpes simplex viruses and animal alphaherpesviruses into cells. Rev. Med. Virol. **10:**305–319.
5. **Campadelli-Fiume, G., S. Qi, E. Avitabile, L. Foà-Tomasi, R. Brandimarti, and B. Roizman.** 1990. Glycoprotein D of herpes simplex virus encodes a domain which precludes penetration of cells expressing the glycoprotein by superinfecting herpes simplex virus. J. Virol. **64:**6070–6079.
6. **Carfi, A., S. H. Willis, J. C. Whitbeck, C. Krummenacher, G. H. Cohen, R. J. Eisenberg, and D. C. Wiley.** 2001. Herpes simplex virus glycoprotein D bound to the human receptor HveA. Mol. Cell **8:**169–179.
7. **Chiang, H.-Y., G. H. Cohen, and R. J. Eisenberg.** 1994. Identification of functional regions of herpes simplex virus glycoprotein gD by using linker-insertion mutagenesis. J. Virol. **68:**2529–2543.
8. **Clackson, T., and J. A. Wells.** 1995. A hot spot of binding energy in a hormone-receptor interface. Science **267:**383–386.
9. **Cocchi, F., D. Fusco, L. Menotti, T. Gianni, R. J. Eisenberg, G. H. Cohen, and G. Campadelli-Fiume.** 2004. The soluble ectodomain of herpes simplex virus gD contains a membrane-proximal pro-fusion domain and suffices to mediate virus entry. Proc. Natl. Acad. Sci. USA **101:**7445–7450.
10. **Cohen, G. H., B. Dietzschold, M. Ponce de Leon, D. Long, E. Golub, A. Varrichio, L. Pereira, and R. J. Eisenberg.** 1984. Localization and synthesis of an antigenic determinant of herpes simplex virus glycoprotein D that stimulates production of neutralizing antibody. J. Virol. **49:**102–108.
11. **Cohen, G. H., V. J. Isola, J. Kuhns, P. W. Berman, and R. J. Eisenberg.** 1986. Localization of discontinuous epitopes of herpes simplex virus glycoprotein D: use of a nondenaturing ("native" gel) system of polyacrylamide gel electrophoresis coupled with Western blotting. J. Virol. **60:**157–166.
12. **Connolly, S. A., D. J. Landsburg, A. Carfi, D. C. Wiley, G. H. Cohen, and R. J. Eisenberg.** 2003. Structure-based mutagenesis of herpes simplex virus glycoprotein D defines three critical regions at the gD/HveA interface. J. Virol. **77:**8127–8140.
13. **Connolly, S. A., D. J. Landsburg, A. Carfi, D. C. Wiley, R. J. Eisenberg, and G. H. Cohen.** 2002. Structure-based analysis of the herpes simplex virus glycoprotein D binding site present on herpesvirus entry mediator HveA. J. Virol. **76:**10894–10904.
14. **Connolly, S. A., J. C. Whitbeck, A. H. Rux, C. Krummenacher, S. van Drunen Littel-van den Hurk, G. H. Cohen, and R. J. Eisenberg.** 2001. Glycoprotein D homologues in herpes simplex virus type 1, pseudorabies virus, and bovine herpes virus type 1 bind directly to human HveC (nectin-1) with different affinities. Virology **280:**7–18.
15. **Dean, H. J., S. S. Terhune, M. Shieh, N. Susmarski, and P. G. Spear.** 1994. Single amino acid substitutions in gD of herpes simplex virus 1 confer resistance to gD-mediated interference and cause cell-type-dependent alterations in infectivity. Virology **199:**67–80.
16. **Eisenberg, R. J., D. Long, M. Ponce de Leon, J. T. Matthews, P. G. Spear, M. G. Gibson, L. A. Lasky, P. Berman, E. Golub, and G. H. Cohen.** 1985. Localization of epitopes of herpes simplex virus type 1 glycoprotein D. J. Virol. **53:**634–644.
17. **Fan, Q. R., E. O. Long, and D. C. Wiley.** 2000. A disulfide-linked natural killer cell receptor dimer has higher affinity for HLA-C than wild-type monomer. Eur. J. Immunol. **30:**2692–2697.
18. **Farzan, M., H. Choe, E. Desjardins, Y. Sun, J. Kuhn, J. Cao, D. Archambault, P. Kolchinsky, M. Koch, R. Wyatt, and J. Sodroski.** 1998. Stabilization of human immunodeficiency virus type 1 envelope glycoprotein trimers by disulfide bonds introduced into the gp41 glycoprotein ectodomain. J. Virol. **72:**7620–7625.
19. **Friedman, H. M., G. H. Cohen, R. J. Eisenberg, C. A. Seidel, and D. B. Cines.** 1984. Glycoprotein C of herpes simplex virus 1 acts as a receptor for the C3b component of complement on infected cells. Nature **309:**633–635.
20. **Fuller, A. O., and W. C. Lee.** 1992. Herpes simplex virus type 1 entry through a cascade of virus-cell interactions requires different roles of gD and gH in penetration. J. Virol. **66:**5002–5012.
21. **Geraghty, R. J., C. R. Jogger, and P. G. Spear.** 2000. Cellular expression of alphaherpesvirus gD interferes with entry of homologous and heterologous alphaherpesviruses by blocking access to a shared gD receptor. Virology **268:**147–158.
22. **Geraghty, R. J., C. Krummenacher, R. J. Eisenberg, G. H. Cohen, and P. G. Spear.** 1998. Entry of alphaherpesviruses mediated by poliovirus receptor related protein 1 and poliovirus receptor. Science **280:**1618–1620.
23. **Godley, L., J. Pfeifer, D. Steinhauer, B. Ely, G. Shaw, R. Kaufmann, E. Suchanek, C. Pabo, J. J. Skehel, D. C. Wiley, et al.** 1992. Introduction of intersubunit disulfide bonds in the membrane-distal region of the influenza hemagglutinin abolishes membrane fusion activity. Cell **68:**635–645.
24. **Guex, N., and M. C. Peitsch.** 1997. SWISS-MODEL and the Swiss-Pdb-Viewer: an environment for comparative protein modeling. Electrophoresis **18:**2714–2723.
25. **Handler, C. G., G. H. Cohen, and R. J. Eisenberg.** 1996. Cross-linking of glycoprotein oligomers during herpes simplex virus type 1 entry. J. Virol. **70:**6076–6082.
26. **Holland, T. C., S. D. Marlin, M. Levine, and J. Glorioso.** 1983. Antigenic variants of herpes simplex virus selected with glycoprotein-specific monoclonal antibodies. J. Virol. **45:**672–682.

27. **Huber, M. T., T. W. Wisner, N. R. Hegde, K. A. Goldsmith, D. A. Rauch, R. J. Roller, C. Krummenacher, R. J. Eisenberg, G. H. Cohen, and D. C. Johnson.** 2001. Herpes simplex virus with highly reduced gD levels can efficiently enter and spread between human keratinocytes. J. Virol. **75:**10309–10318.
28. **Isola, V. J., R. J. Eisenberg, G. R. Siebert, C. J. Heilman, W. C. Wilcox, and G. H. Cohen.** 1989. Fine mapping of antigenic site II of herpes simplex virus glycoprotein D. J. Virol. **63:**2325–2334.
29. **Jogger, C. R., R. I. Montgomery, and P. G. Spear.** 2004. Effects of linker-insertion mutations in herpes simplex virus 1 gD on glycoprotein-induced fusion with cells expressing HVEM or nectin-1. Virology **318:**318–326.
30. **Krummenacher, C., F. Baribaud, M. Ponce De Leon, I. Baribaud, J. C. Whitbeck, R. Xu, G. H. Cohen, and R. J. Eisenberg.** 2004. Comparative usage of herpesvirus entry mediator A and nectin-1 by laboratory strains and clinical isolates of herpes simplex virus. Virology **322:**286–299.
31. **Krummenacher, C., A. V. Nicola, J. C. Whitbeck, H. Lou, W. Hou, J. D. Lambris, R. J. Geraghty, P. G. Spear, G. H. Cohen, and R. J. Eisenberg.** 1998. Herpes simplex virus glycoprotein D can bind to poliovirus receptor-related protein 1 or herpesvirus entry mediator, two structurally unrelated mediators of virus entry. J. Virol. **72:**7064–7074.
32. **Krummenacher, C., A. H. Rux, J. C. Whitbeck, M. Ponce de Leon, H. Lou, I. Baribaud, W. Hou, C. Zou, R. J. Geraghty, P. G. Spear, R. J. Eisenberg, and G. H. Cohen.** 1999. The first immunoglobulin-like domain of HveC is sufficient to bind herpes simplex virus gD with full affinity while the third domain is involved in oligomerization of HveC. J. Virol. **73:**8127–8137.
33. **Kwon, B. S., K. B. Tan, J. Ni, K. O. Oh, Z. H. Lee, K. K. Kim, Y. J. Kim, S. Wang, R. Gentz, G.-L. Yu, J. Harrop, S. D. Lyn, C. Silverman, T. G. Porter, A. Truneh, and P. R. Young.** 1997. A newly identified member of the tumor necrosis factor receptor superfamily with a wide tissue distribution and involvement in lymphocyte activation. J. Biol. Chem. **272:**14272–14276.
34. **Ligas, M. W., and D. C. Johnson.** 1988. A herpes simplex virus mutant in which glycoprotein D sequences are replaced by β-galactosidase sequences binds to but is unable to penetrate into cells. J. Virol. **62:**1486–1494.
35. **Lopez, M., F. Cocchi, E. Avitabile, A. Leclerc, J. Adelaide, G. Campadelli-Fiume, and P. Dubreuil.** 2001. Novel, soluble isoform of the herpes simplex virus (HSV) receptor nectin1 (or PRR1-HIgR-HveC) modulates positively and negatively susceptibility to HSV infection. J. Virol. **75:**5684–5691.
36. **Lopez, M., F. Cocchi, L. Menotti, E. Avitabile, P. Dubreuil, and G. Campadelli-Fiume.** 2000. Nectin2α (PRR2α or HveB) and nectin2δ are low-efficiency mediators for entry of herpes simplex virus mutants carrying the Leu25Pro substitution in glycoprotein D. J. Virol. **74:**1267–1274.
37. **Mauri, D. N., R. Ebner, K. D. Kochel, R. I. Montgomery, T. C. Cheung, G.-L. Yu, M. Murphy, R. J. Eisenberg, G. H. Cohen, P. G. Spear, and C. F. Ware.** 1998. LIGHT, a new member of the TNF superfamily, and lymphotoxin (LT) α are ligands for herpesvirus entry mediator (HVEM). Immunity **8:**21–30.
38. **Menotti, L., E. Avitabile, P. Dubreuil, M. Lopez, and G. Campadelli-Fiume.** 2001. Comparison of murine and human nectin1 binding to herpes simplex virus glycoprotein D (gD) reveals a weak interaction of murine nectin1 to gD and a gD-dependent pathway of entry. Virology **282:**256–266.
39. **Miller, C. G., C. Krummenacher, R. J. Eisenberg, G. H. Cohen, and N. W. Fraser.** 2001. Development of a syngenic murine B16 cell line-derived melanoma susceptible to destruction by neuroattenuated HSV-1. Mol. Ther. **3:**160–168.
40. **Milne, R. S. B., S. A. Connolly, C. Krummenacher, R. J. Eisenberg, and G. H. Cohen.** 2001. Porcine HveC, a member of the highly conserved HveC/nectin 1 family, is a functional alphaherpesvirus receptor. Virology **281:**315–328.
41. **Milne, R. S. B., S. L. Hanna, A. H. Rux, S. H. Willis, G. H. Cohen, and R. J. Eisenberg.** 2003. Function of herpes simplex virus type 1 gD mutants with different receptor-binding affinities in virus entry and fusion. J. Virol. **77:**8962–8972.
42. **Minson, A. C., T. C. Hodgman, P. Digard, D. C. Hancock, S. E. Bell, and E. A. Buckmaster.** 1986. An analysis of the biological properties of monoclonal antibodies against glycoprotein D of herpes simplex virus and identification of amino acid substitutions that confer resistance to neutralization. J. Gen. Virol. **67:**1001–1013.
43. **Montgomery, R. I., M. S. Warner, B. J. Lum, and P. G. Spear.** 1996. Herpes simplex virus-1 entry into cells mediated by a novel member of the TNF/NGF receptor family. Cell **87:**427–436.
44. **Muggeridge, M. I., V. J. Isola, R. A. Byrn, T. J. Tucker, A. C. Minson, J. C. Glorioso, G. H. Cohen, and R. J. Eisenberg.** 1988. Antigenic analysis of a major neutralization site of herpes simplex virus glycoprotein D, using deletion mutants and monoclonal antibody-resistant mutants. J. Virol. **62:**3274–3280.
45. **Muggeridge, M. I., S. R. Roberts, V. J. Isola, G. H. Cohen, and R. J. Eisenberg.** 1990. Herpes simplex virus, p. 459–481. *In* M. H. V. van Regenmortel and A. R. Neurath (ed.), Immunochemistry of viruses, vol. II. The basis for serodiagnosis and vaccines. Elsevier Biochemical Press, Amsterdam, The Netherlands.
46. **Muggeridge, M. I., T.-T. Wu, D. C. Johnson, J. C. Glorioso, R. J. Eisenberg, and G. H. Cohen.** 1990. Antigenic and functional analysis of a neutralization site of HSV-1 glycoprotein D. Virology **174:**375–387.
47. **Nicola, A. V., M. Ponce de Leon, R. Xu, W. Hou, J. C. Whitbeck, C. Krummenacher, R. I. Montgomery, P. G. Spear, R. J. Eisenberg, and G. H. Cohen.** 1998. Monoclonal antibodies to distinct sites on the herpes simplex virus (HSV) glycoprotein D block HSV binding to HVEM. J. Virol. **72:**3595–3601.
48. **Nicola, A. V., S. H. Willis, N. N. Naidoo, R. J. Eisenberg, and G. H. Cohen.** 1996. Structure-function analysis of soluble forms of herpes simplex virus glycoprotein D. J. Virol. **70:**3815–3822.
49. **Okuma, K., M. Nakamura, S. Nakano, Y. Niho, and Y. Matsuura.** 1999. Host range of human T-cell leukemia virus type I analyzed by a cell fusion-dependent reporter gene activation assay. Virology **254:**235–244.
50. **Pereira, L., T. Klassen, and J. R. Baringer.** 1980. Type-common and type-specific monoclonal antibody to herpes simplex virus type 1. Infect. Immun. **29:**724–732.
51. **Pertel, P. E., A. Fridberg, M. L. Parish, and P. G. Spear.** 2001. Cell fusion induced by herpes simplex virus glycoproteins gB, gD, and gH-gL requires a gD receptor but not necessarily heparan sulfate. Virology **279:**313–324.
52. **Richart, S. M., S. A. Simpson, C. Krummenacher, J. C. Whitbeck, L. I. Pizer, G. H. Cohen, R. J. Eisenberg, and C. L. Wilcox.** 2003. Entry of herpes simplex virus type 1 into primary sensory neurons in vitro is mediated by nectin-1/HveC. J. Virol. **77:**3307–3311.
53. **Spear, P. G., R. J. Eisenberg, and G. H. Cohen.** 2000. Three classes of cell surface receptors for alphaherpesvirus entry. Virology **275:**1–8.
54. **Spear, P. G., and R. Longnecker.** 2003. Herpesvirus entry: an update. J. Virol. Methods **77:**10179–10185.
55. **Takahashi, K., H. Nakanishi, M. Miyahara, K. Mandai, K. Satoh, A. Satoh, H. Nishioka, J. Aoki, A. Nomoto, A. Mizoguchi, and Y. Takai.** 1999. Nectin/PRR: an immunoglobulin-like cell adhesion molecule recruited to cadherin-based adherens junctions through interaction with afadin, a PDZ domain-containing protein. J. Cell Biol. **145:**539–549.
56. **Takai, Y., and H. Nakanishi.** 2003. Nectin and afadin: novel organizers of intercellular junctions. J. Cell Sci. **116:**17–27.
57. **Terry-Allison, T., R. I. Montgomery, J. C. Whitbeck, R. Xu, G. H. Cohen, R. J. Eisenberg, and P. G. Spear.** 1998. HveA (herpesvirus entry mediator A), a coreceptor for herpes simplex virus entry, also participates in virus-induced cell fusion. J. Virol. **72:**5802–5810.
58. **Thornton, J. M.** 1981. Disulphide bridges in globular proteins. J. Mol. Biol. **151:**261–287.
59. **Turner, A., B. Bruun, T. Minson, and H. Browne.** 1998. Glycoproteins gB, gD, and gHgL of herpes simplex virus type 1 are necessary and sufficient to mediate membrane fusion in a Cos cell transfection system. J. Virol. **72:**873–875.
60. **Warner, M. S., W. Martinez, R. J. Geraghty, R. I. Montgomery, J. C. Whitbeck, R. Xu, R. J. Eisenberg, G. H. Cohen, and P. G. Spear.** 1998. A cell surface protein with herpesvirus entry activity (HveB) confers susceptibility to infection by herpes simplex virus type 2, mutants of herpes simplex virus type 1 and pseudorabies virus. Virology **246:**179–189.
61. **Wells, J. A.** 1991. Systematic mutational analyses of protein-protein interfaces. Methods Enzymol. **202:**390–411.
62. **Whitbeck, J. C., S. A. Connolly, S. H. Willis, W. Hou, C. Krummenacher, M. Ponce de Leon, H. Lou, I. Baribaud, R. J. Eisenberg, and G. H. Cohen.** 2001. Localization of the gD-binding region of the human herpes simplex virus receptor, HveA. J. Virol. **75:**171–180.
63. **Whitbeck, J. C., M. I. Muggeridge, A. Rux, W. Hou, C. Krummenacher, H. Lou, A. van Geelen, R. J. Eisenberg, and G. H. Cohen.** 1999. The major neutralizing antigenic site on herpes simplex virus glycoprotein D overlaps a receptor-binding domain. J. Virol. **73:**9879–9890.
64. **Whitbeck, J. C., C. Peng, H. Lou, R. Xu, S. H. Willis, M. Ponce de Leon, T. Peng, A. V. Nicola, R. I. Montgomery, M. S. Warner, A. M. Soulika, L. A. Spruce, W. T. Moore, J. D. Lambris, P. G. Spear, G. H. Cohen, and R. J. Eisenberg.** 1997. Glycoprotein D of herpes simplex virus (HSV) binds directly to HVEM, a member of the TNFR superfamily and a mediator of HSV entry. J. Virol. **71:**6083–6093.
65. **Willis, S. H., A. H. Rux, C. Peng, J. C. Whitbeck, A. V. Nicola, H. Lou, W. Hou, L. Salvador, G. H. Cohen, and R. J. Eisenberg.** 1998. Examination of the kinetics of herpes simplex virus glycoprotein D binding to the herpesvirus entry mediator, using surface plasmon resonance. J. Virol. **72:**5937–5947.
66. **WuDunn, D., and P. G. Spear.** 1989. Initial interaction of herpes simplex virus with cells is binding to heparan sulfate. J. Virol. **63:**52–58.
67. **Yoon, M., and P. G. Spear.** 2002. Disruption of adherens junctions liberates nectin-1 to serve as receptor for herpes simplex virus and pseudorabies virus entry. J. Virol. **76:**7203–7208.
68. **Yoon, M., A. Zago, D. Shukla, and P. G. Spear.** 2003. Mutations in the N termini of herpes simplex virus type 1 and 2 gDs alter functional interactions with the entry/fusion receptors HVEM, nectin-2, and 3-*O*-sulfated heparan sulfate but not with nectin-1. J. Virol. **77:**9221–9231.
69. **Zhou, G., E. Avitabile, G. Campadelli-Fiume, and B. Roizman.** 2003. The domains of glycoprotein D required to block apoptosis induced by herpes simplex virus 1 are largely distinct from those involved in cell-cell fusion and binding to nectin1. J. Virol. **77:**3759–3767.
70. **Zhou, G., G. J. Ye, W. Debinski, and B. Roizman.** 2002. Engineered herpes simplex virus 1 is dependent on IL13Rα2 receptor for cell entry and independent of glycoprotein D receptor interaction. Proc. Natl. Acad. Sci. USA **99:**15124–15129.